Mendeleev Communications

Focus Article, *Mendeleev Commun.*, 2026, **36**, 1–11

Design and biomedical applications of fluorescent probes based on hemicyanine dyes

Mariya A. Ustimova* and Olga A. Fedorova

A. N. Nesmeyanov Institute of Organoelement Compounds, Russian Academy of Sciences, 119334 Moscow, Russian Federation. E-mail: ustimova@ineos.ac.ru

DOI: 10.71267/mencom.7826

In recent years, fluorescence-based methods have been extensively used to analyze biological processes and to develop medical diagnostic systems. Small molecules, primarily dyes, are commonly used as fluorescent reagents. This review focuses on hemicyanine dyes and their application as fluorophores in biomedical research. These compounds exhibit high affinity for biological molecules, which explains their widespread use for staining nucleic acids and cellular organelles such as mitochondria, lysosomes, endoplasmic reticulum, and nuclei. Examples of hemicyanines used for detecting pathological conditions, including mitophagy, β-amyloid aggregation, and others are also provided.

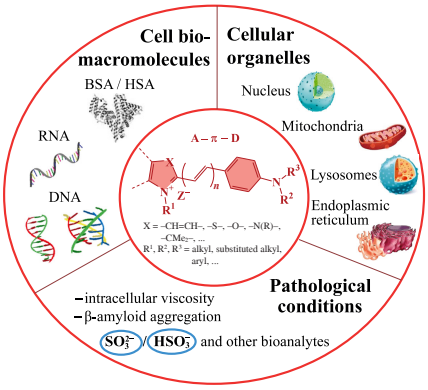

Keywords: hemicyanine dyes, styryl dyes, polymethine dyes, fluorescent sensor, bioimaging, DNA, RNA, mitochondria, lysosomes, β-amyloid, endoplasmic reticulum, BSA, HSA.

In recent years, significant attention has been brought to the development of new fluorescence-based research methods in molecular and cellular biology, biomedicine, and biophysics. One of the main reasons for this is the sensitivity of fluorescence techniques that often surpasses not only the sensitivity of methods based on light absorption but also that of approaches utilizing radioactive isotopes. Indeed, modern instruments and methodologies enable detection of fluorescence signals even from individual molecules, which has led to the emergence and development of single-molecule fluorescence spectroscopy, a method widely employed to study individual molecules in dynamics.[1] For biophysicists, fluorescence has become a rapid and sensitive tool for investigating the structure, dynamics, and functions of nucleic acids[2] and proteins.[3] Fluorescence has provided new impetus to the development of cellular biology owing to confocal fluorescence microscopy and creation of novel fluorescent probes. It has also enabled detailed analysis of the chemical composition of living cells and even organisms, as well as its changes over time and space, giving rise to the foundation of fluorescent molecular imaging.[4,5]

The main classes of fluorescent probes include organic dyes, lanthanide coordination compounds, fluorescent proteins, and semiconductor nanocrystals. Each class has its own specific features, advantages, and drawbacks. Small fluorescent molecules provide an indispensable tool in biology and are widely used as molecular probes, environmental indicators, and cellular dyes.[6–8] Selecting an appropriate fluorophore for visualizing a biochemical or biological process can be challenging, given the large number of molecules available either commercially or through *de novo* design and synthesis.

For the successful use of organic dyes as fluorescent markers, they must possess high fluorescence quantum yields and molar extinction coefficients. Dyes with narrow luminescence bands are also preferable, especially for instruments with channel-

Mariya A. Ustimova was born in Southern Urals of Russia, in 1994. She obtained her BSc degree in 2016 and MSc degree in 2018 at Department of Chemistry and Technology of Biomedical Drugs, D. I. Mendeleev Russian University of Chemical Technology. She received her PhD degree in 2023 at A. N. Nesmeyanov Institute of Organoelement Compounds of Russian Academy of Sciences. Her research interest includes synthesis and application of styryl dye derivatives in bioimaging.

Olga A. Fedorova was born in Moscow, Russia. After study at Chemistry Department of Moscow State University where she got a diploma and PhD in Organic Chemistry (Rearrangements in Adamantyl Derivatives), she was recruited in Prof. M. Alfimov's group (Photochemistry Center of Russian Academy of Sciences) as a Senior Researcher. Her interest moved to supramolecular organic photoactive systems. She obtained the Doctor degree in this field. Now she is a head of Laboratory of Photoactive Supramolecular Systems at the A. N. Nesmeyanov Institute of Organoelement Compounds of Russian Academy of Sciences and Professor of Moscow State University and D. I. Mendeleev Russian University of Chemical Technology where she gives lectures on Supramolecular Chemistry. She is a co-author of more than 300 papers.

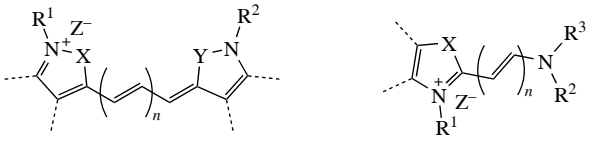

X, Y = CH=CH, S, O, N(R), CMe_2, *etc.*
R^1, R^2, R^3 = alkyl, substituted alkyl, aryl, *etc.*

Figure 1 General structure of cyanine and hemicyanine dyes.

based signal recording, and those intended for use in multiplexed analyses. Logically, in addition to photophysical requirements, fluorescent markers must exhibit sufficient photostability and inertness in aqueous and physiological media and, in some cases, at elevated temperatures. Moreover, it is desirable that the dye withstand the conditions of the synthetic cycle used for biomolecule labeling.

Hemicyanine dyes, which belong to the subclass of polymethine dyes, represent one of the classes of fluorophores used in biology and medicine. Unlike the classical cyanine dyes, which comprise a conjugated chain of sp^2-hybridized carbon atoms connecting two terminal nitrogen atoms, each of them forming unsaturated heterocycles jointly with parts of the conjugated chain, hemicyanine dyes contain two terminal groups differing in nature (Figure 1).[9] The structure of hemicyanine dyes involves a polymethine chain with an acceptor heterocyclic moiety at one end and an aromatic donor moiety, which is not part of the unsaturated heterocyclic system, at the other end.[9]

Advantages of hemicyanine dyes include the ease of their synthesis and availability of starting reagents. The main approach to the preparation of such compounds involves a two-step synthesis, where a quaternary ammonium salt is obtained at the first step by quaternization of an *N*-containing heterocycle, and the salt is then subjected to the Knoevenagel condensation with the corresponding carbonyl derivative (Figure 2).[10,11] Thus, it is possible to obtain a number of dyes with absorption and emission in a wide spectral range by varying the structure of heterocycles and substituents in the structure of the starting reagents, as well as by elongation of the polymethine chain.

The class of hemicyanine dyes is widely known as dyes with intramolecular charge transfer (ICT). The structure of these dyes contains strong donor moieties for destabilization of ground state potentials and acceptor groups for stabilization of excited state potentials.[12] The addition of each methine link to the polymethine bridge of such dyes can provide a significant bathochromic shift. Due to their easy-to-modify structure, varying the substituents in hemicyanine dyes allows shifting the absorption and emission wavelength maxima down to the near-infrared range.[13–16] This is particularly important in biological applications, since some tissues and biomolecules produce autofluorescence between 200 and 650 nm and thus may affect the fluorescence image quality of a short-wavelength probe.

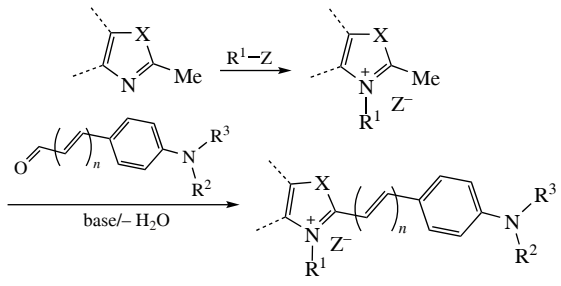

X = CH=CH, S, O, N(R), CMe_2, *etc.*
R^1, R^2, R^3 = alkyl, substituted alkyl, aryl, *etc.*
n = 0, 1, 2

Figure 2 General scheme for the synthesis of hemicyanine dyes.

Another advantage of hemicyanine dyes is their high photostability compared to classical cyanine dyes, which is particularly important in biovisualization applications.[17–21]

In the fields of biology and medicine, hemicyanines have found application as dyes that bind to biological molecules in a non-covalent way. The high affinity of hemicyanine dyes to biomolecules distinguishes them from closely related cyanine dyes which show weak association with biomolecules and are widely used for covalent labeling of biomolecules. Another property that explains the use of hemicyanines for non-covalent binding to biomolecules is their ability to change their fluorescence in a biological environment. Such dyes fluoresce weakly in a free, non-immobilized state due to the presence of channels for radiation-free relaxation of the excited state, such as the formation of non-fluorescent Twisted Intramolecular Charge Transfer (TICT) states in polar media or *E*–*Z*-isomerization at the double C=C bond. In both cases, fluorescence enhancement can be observed in biomolecule cavities that can impede internal rotation or isomerization. Therefore, these probes can often be used without a washing step to remove excess fluorescent dyes after staining a biological object.

Within the framework of this review, we tried to collect the most interesting examples of studies on hemicyanine dyes as fluorescent markers for biomedical research. We divided dyes of this type into two main groups, styryl and polymethine dyes. This division allows us to trace the effect of structural factors on the optical characteristics and peculiarities of the interaction with biomolecules within each group.

The review also focuses on examples of the use of hemicyanine dyes as fluorophores for staining organelles and nucleic acids. Fluorescent dyes are used in fluorescence microscopy to visualize the localization and distribution of cellular structures of interest. This provides important information about the functional state and morphology of the cells being studied. Vital (live-cell) dyes make it possible to trace dynamic changes in cells in real time. For example, one can observe the movement of organelles, transport of vesicles, reorganization of the cytoskeleton, and other intracellular processes. To examine the above-mentioned processes, it is important to synthesize fluorophores that have specific distribution in such important cellular components as nuclei, membranes, lysosomes, mitochondria, cytoskeleton, endoplasmic reticulum.

Fluorophores specific for binding to nucleic acids are designed to support diagnostic methods and develop new drugs. Fluorescent markers are used to study structural and conformational polymorphisms of nucleic acids (NAs), their variability and internal dynamics, their interaction with proteins, metabolites, drugs targeting NAs, water molecules and ions at the submolecular and atomic levels.[22–24] Therefore, many synthesized fluorophores are studied for their interaction with nucleic acids.

Styryl dyes

Styryl dyes are the structurally simplest hemicyanines containing only one double bond in the linker structure. Small changes in the structure of styryl dyes can affect significantly not only their optical properties, but also their interaction with biomolecules and localization within the cell. Many researchers attempt to identify direct structure–property relationships in the series of styryl dyes to create a fluorescent agent with desired parameters. In this regard, this chapter will review the recent studies on styryl dyes with various structures containing the most popular moieties, such as benzothiazole, carbazole, quinoline, naphthyridine, and others.

The effect of the nature of substituents in the aryl ring of styryl dyes has been studied using synthesized dyes of the

benzothiazolium series as an example. Benzothiazolium dyes offer advantages such as high biocompatibility, rapid penetration into intracellular environment, high photostability, and stability in solution, which account for their widespread use in studies published over the past decade. The scientific team led by C. S. Abeywickrama[25] using the synthesized series of dyes **1**–**3** as an example (Figure 3) found that the dyes had broad absorption and emission bands ($\lambda_{max}^{abs} \approx 405$ nm; $\lambda_{max}^{fluor} \approx 510$ nm in H_2O), while the fluorescence quantum yields of probes **1** and **3** depended on the type of donor substituent. For example, dye **1** (–OH donor; $\varphi^{fluor} \approx 0.0002$ in H_2O) showed a higher fluorescence quantum yield than probe **3** (–OMe donor; $\varphi^{fluor} \approx 0.0001$ in H_2O). In studies on cells, it was found that the presence of a donor group such as OH or OMe promoted specific localization of the dye in lysosomes.[25]

Using the data obtained from the experiments that confirmed the lysosomal selectivity of dyes **1**–**3**, the authors[26] tried to substantiate how the nature of the donor group (D) in the aryl moiety of a styryl benzothiazole dye could contribute to the specificity of organelle staining. To do so, morpholine being a well-established guide group for lysosomes[27] was bound with the aryl moiety of styryl (compound **4**, see Figure 3). Interestingly, the study of the localization of dye **4** in MO3.13 and NHLF cells by fluorescence confocal microscopy showed that the dye simultaneously stained both cellular lysosomes and mitochondria. The observed dual selectivity of probe **4** can be explained by the well-established ability of the morpholine moiety to target lysosomes,[27] while the mitochondrial selectivity can be attributed to the effect of the donor properties of morpholine as a substituent at the aryl moiety of styryl **4**.[28]

To confirm the effect of the donor moiety in the D–π–A chromophore system on the specificity of binding to organelles, dyes **5** and **6** (see Figure 3) containing aromatic diphenylamine as a substituent that has a small donor effect were synthesized.[29] In contrast to dyes **1**–**4**, significantly different photophysical properties and selectivity toward organelles were observed for compounds **5** and **6**. Probes **5** and **6** showed almost no fluorescence in many polar and nonpolar solvents but exhibited bright red fluorescence ($\lambda_{max}^{fluor} \approx 630$–$640$ nm) in stained MO3.13 and NHLF cells at very low probe concentrations (~200 nM). Co-localization studies based on fluorescence confocal microscopy revealed the excellent lysosomal selectivity of probes **5** and **6**. The photostability of the dyes was found to depend on the substituent (R′) at the quaternary nitrogen atom: the derivative with a benzyl substituent (**6**) demonstrated greater photostability compared to that with a methyl substituent (**5**). The described dyes also showed significant fluorescence enhancement upon interaction with albumin.[30] The authors suggested that an increase in fluorescence intensity of compounds **5** and **6** upon localization in cellular lysosomes is related to the interactions with intracellular biomolecules.

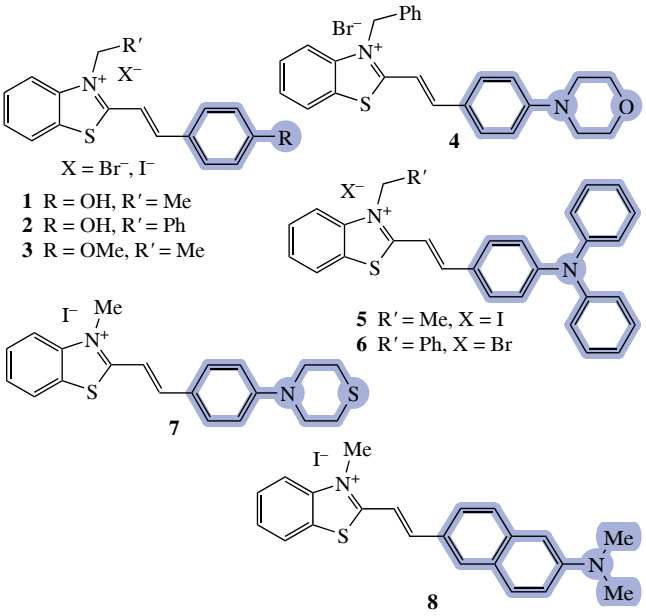

Figure 3 Structures of styryl dyes **1**–**8** containing a benzothiazolium moiety.

Another interesting example of structural modification of a benzothiazolium dye was presented in an article where the thiomorpholine fragment was used as a donor of the chromophore system.[31] Dye **7** (see Figure 3) had a broad absorption band with a maximum at 490 nm and an emission spectrum with a maximum at 590 nm. In a buffer solution, the dye had a low fluorescence quantum yield, which increased significantly (almost tenfold) in the presence of double-stranded DNA. Biological experiments showed that the dye freely passed through the cell membrane and did not cause cell death. After penetrating into a cell, the dye targets the nucleoli and endoplasmic reticulum of the cell.

Mitochondria-targeted fluorescent benzothiazolium near-infrared (NIR) dye **8** (see Figure 3) was presented in ref. 32 where, in addition to live cell imaging, the probe was used for the ratiometric detection of SO_2 derivatives. Detection occurred due to SO_2 addition to the double bond in the dye through the Michael reaction (Scheme 1). The probe showed an ultrafast response time (within 10 s), a large hypochromic shift (260 nm), high photostability, excellent selectivity, and high sensitivity in aqueous media with a detection limit of 43 nM. Intracellular imaging results indicated that probe **8** targets mitochondria and can be used for the detection of both exogenous and endogenous SO_2 derivatives in living cells.

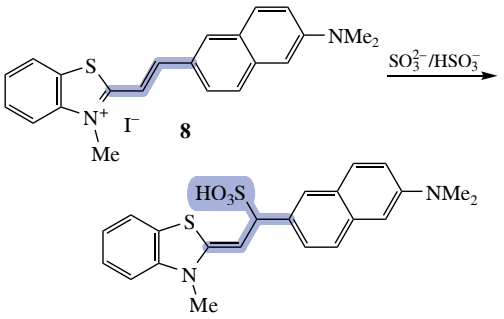

Scheme 1

To find the optimal probes for HSO_3^-, a team of Chinese scientists[33] synthesized four fluorescent hemicyanine dyes **9**–**12** containing hydroxyaryl moieties (Figure 4). Like for dye **8**, HSO_3^- detection was inplemented at the double bond by the Michael reaction. Despite the similarity of structures, dyes **9**–**12** showed different effects. Dye **12** demonstrated the weakest response due to the donor properties of indole, which does not favor the nucleophilic addition of HSO_3^-. Another distinctive feature is that dye **10** did not exhibit selective localization in cell mitochondria, which can be explained by the formation of an intramolecular salt between the positively charged azaheterocyclic moiety and propanesulfonic acid group. This neutralizes the overall positive charge of the molecule, thus the molecule is capable of localization in mitochondria. Based on the results of spectrophotometric and spectrofluorimetric titrations, the limits for detection of HSO_3^- for dye **9** were 2.308 μM (as calculated from the absorption spectra) and 0.844 μM (as calculated from the fluorescence spectra). The results of these studies showed that dye **9** can be used for the detection of exogenous and endogenous HSO_3^- in living cells.

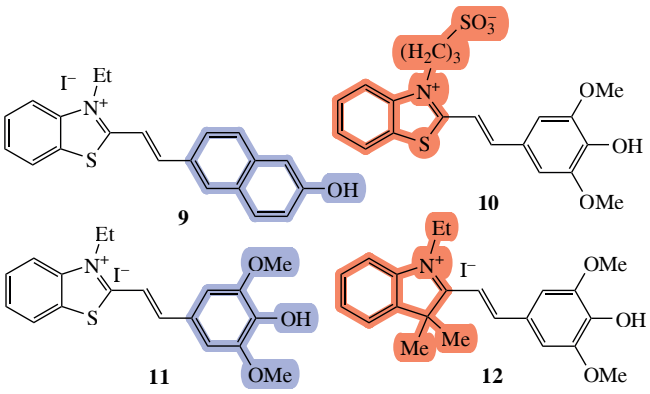

Figure 4 Structures of styryl dyes **9**–**12** containing a hydroxyaryl moiety.

Further studies of dye **11** (see Figure 4) revealed[34] that this dye could be also successfully used to detect the changes in the mitochondrial microenvironment in cardiomyocytes (cardiac muscle cells) caused by the presence of Zn^{2+} cations. Dye **11** was also found to be sensitive to pH changes. Moreover, it was detected both in a cell nucleus and mitochondria, which is advantageous for visualizing the overall cell morphology.

Mitochondria, the primary organelles responsible for cellular energy production and regulation of cell behavior, play a crucial role in various diseases, particularly cancer. Fluorophores targeting mitochondria make it possible to monitor morphological changes, functional integrity and mitochondrial defects. Monitoring mitochondrial viscosity is an important aspect of observing the process of mitophagy (selective degradation of mitochondria) in real time. Consequently, the development of high-throughput viscosity probes is essential for investigating the dynamic pathological processes in mitochondria associated with mitophagy. A team of researchers from China[35] has developed two neutral hemicyanine dyes **13**, **14** (Figure 5). The dyes comprise a quinoline or naphthyridine heterocycles, respectively, as the acceptor of the chromophore system and a coumarin moiety as the donor. In different solvents, the dyes exhibited absorption maxima at 433–471 nm and emission maxima at 605–720 nm with large Stokes shifts of 170–279 nm. As the viscosity of the medium was increased from 0.89 to 856 cP, the fluorescence intensity of probes **13** and **14** increased by a factor of 418 and 769, respectively. This effect is explained by the restricted relaxation of the dyes' excited states upon the formation of twisted states in a viscous biological medium. The dyes were then studied as probes for visualization of changes in mitochondrial viscosity during mitophagy due to the addition of rapamycin. The results obtained from the biological experiments showed that dyes **13**, **14** are promising candidates for studies on dynamic pathological processes associated with mitophagy. The compounds exhibited high photostability and resistance to changes in acidity and polarity of the medium.

Three naphthyridine dyes **15**–**17** (see Figure 5) with different donor moieties were examined as sensors for DNA and RNA.[36] The probes demonstrated excellent photostability, retaining more than 95% of the optical density in the absorption spectrum after 5 h of irradiation. The dyes exhibited a significant enhancement of fluorescence intensity, namely 143-fold and 127-fold for dye **16** upon interaction with DNA and RNA, respectively. On binding to biomolecules, the emission wavelength maximum could reach the near-infrared region (661–762 nm) with large Stokes shifts (153–222 nm). In the cell experiments, the dyes showed low toxicity and localization in the mitochondria of fixed cells.

Two naphthyridine dyes **18**, **19** with different substituents in the donor fragment (see Figure 5) were developed for the detection of viscosity changes associated with lysosomal and endoplasmic reticulum stress.[21] A piperazine moiety was introduced into the dye structure for targeting lysosomes, and a tosylpiperazine moiety was introduced to target the endoplasmic reticulum. Dyes **18**, **19** showed broad absorption and emission bands located at 472–492 and 610–664 nm and large Stokes shifts ranging from 136 to 194 nm in different polar solvents. The dyes also exhibited fluorescence sensitivity to the viscosity of the medium, their fluorescence quantum yields in glycerol could reach 63 and 71%. When the viscosity of the medium was increased from 2.08 to 856 cP, the fluorescence intensity of probes **18** and **19** increased 74- and 5.2-fold, respectively. Moreover, dynamic light scattering (DLS) experiments confirmed that probes **18** and **19** exhibited aggregate-induced emission properties. According to the results of imaging experiments in a cellular environment, dye **18** is localized in the lysosome region, while dye **19**, in the endoplasmic reticulum

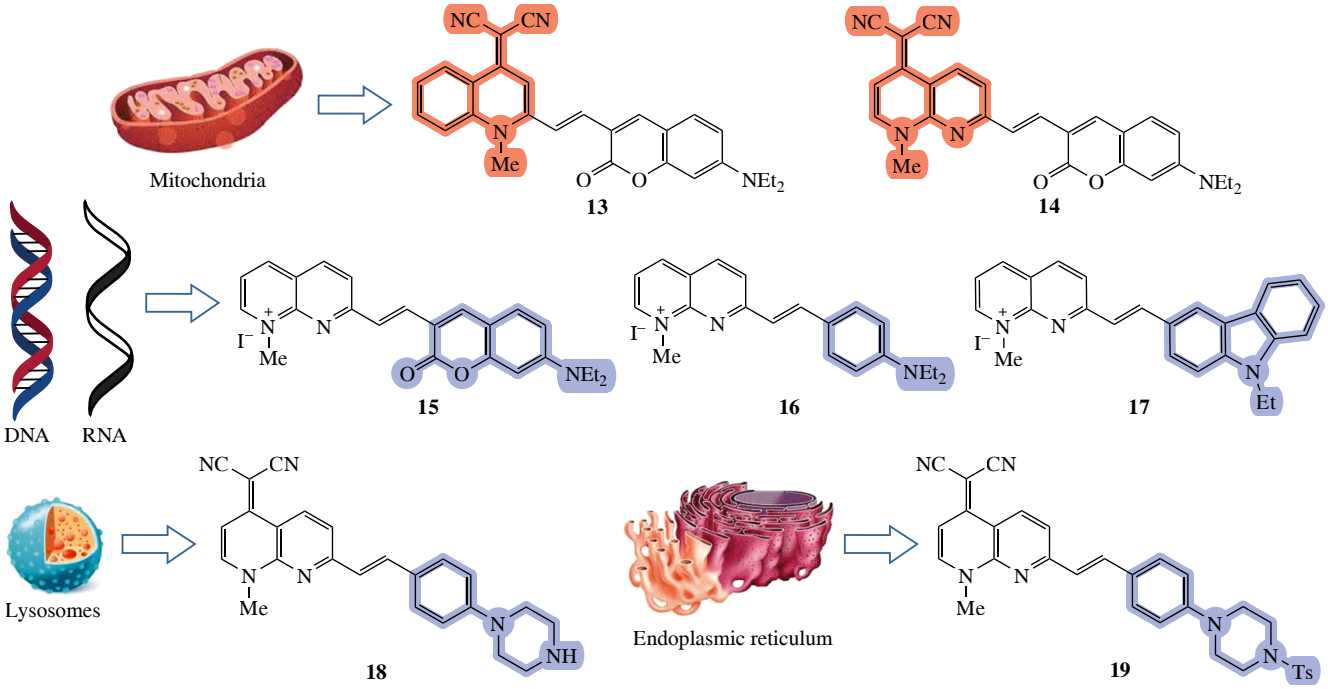

Figure 5 Structures of styryl dyes based on quinoline (**13**) and naphthyridine (**14**–**19**).

region of the cell, which allows precise monitoring of viscosity changes in these organelles. The dyes successfully detected viscosity changes during autophagy and ferroptosis. Moreover, probe **19** demonstrated the ability to migrate from the endoplasmic reticulum to lysosomes upon hydrogen peroxide-induced cellular damage.

Another common structural moiety in the structure of hemicyanine dyes of D–π–A is carbazole, which most often acts as a donor in the chromophore system. The presence of a carbazole moiety causes the formation of twisted photoinduced states within the molecule (TICT-chromophores). The widespread use of carbazole dyes can be attributed to their high affinity for DNA. In 2019, Wei *et al*. reported two new chemosensors **20** and **21** (Figure 6) for DNA detection.[37] Both compounds contained a carbazole moiety modified at position 3, which, as shown previously, stabilized telomeric G-quadruplex DNA.[38,39] In addition, incorporation of substituents can also be a useful strategy, since they may be involved in interactions with NA loops or lodged in the grooves of the G-quadruplex.[40] The fluorescence intensity of probes **20** and **21** increased significantly in the presence of different types of NAs. It is noteworthy that experiments on the cleavage of fluorophore complexes with NA by DNase and RNase showed that dye **20** exhibited a greater selectivity to DNA, while dye **21** could simultaneously bind to both G-quadruplex DNA and RNA. According to the data of experiments on dye co-localization in the cell, probe **20** mainly concentrates in the nucleus, whereas probe **21** predominantly stains the cytoplasm.

Compounds **22** and **23** (see Figure 6) containing carbazole moieties were studied to determine the viscosity in mitochondria.[41] Indolinium moieties in the ligand structures were chosen as the electron acceptor groups. To improve permeability into the cell and to achieve preferential localization of these fluorophores in mitochondria, the nitrogen atom of indolinium was quaternized with bromoethane. A study of the optical properties of the dyes in an ethanol–glycerol solvent mixture confirmed the hypothesis put forward during the design of the structure: increasing the viscosity of the solvent mixture increases the intensity of the fluorescence response. The effect of intracellular cations and anions on the fluorescence response was also studied. It was shown that the presence of these particles in the medium did not result in signal quenching. Finally, biological cell imaging experiments confirmed that the probes were localized in mitochondria and could be used for monitoring changes in viscosity.

G-quadruplex DNAs are widely distributed in the human genome and are involved in many important biological processes. However, many aspects of the mechanism underlying their effect on key biological processes remain to be studied. Therefore, the development of fluorescent probes for the detection of G-quadruplexes is important for basic biological research. In order to develop dyes for the recognition of G-quadruplexes, two carbazole derivatives **24** and **25** comprising methylpyridinium and methylquinolininium as acceptors of the chromophore system (see Figure 6) were synthesized and studied.[42] The results showed that different structurally similar heterocycles exhibited different selectivity toward binding various types of DNA. Dye **24** with a pyridine group can distinguish a G-quadruplex from duplex and single-stranded DNA, since a significant enhancement of its fluorescence was observed in the presence of G-quadruplexes, whereas dye **25** with a quinolinium group showed low selectivity to these DNA types. To confirm the results on the selectivity, sensitivity, and mechanism of binding to G-quadruplex DNA, the properties of dye **24** were further explored by UV-visible spectrophotometry, spectrofluorimetry, circular dichroism (CD), and molecular docking. The CD experiments demonstrated that dye **24** could interact with G-quadruplexes without changing their topology. It was found that dye **24** lodged in the groove region of the G-quadruplex structure and exhibited higher affinity binding to the antiparallel structures of the G-quadruplex. As a result of the studies, several factors important for the development of effective probes for G-quadruplex DNA recognition were identified.

Carbazole dye **26** (see Figure 6) with a quaternized quinolinium moiety in the structure as the acceptor[43] was modified with a phenylboronic acid moiety to increase the efficiency of binding to DNA through hydrogen bonding and π–π-stacking with heterocyclic DNA fragments. The binding affinity and selectivity towards telomeric G-quadruplex DNA were determined by fluorescence spectroscopy, spectrophotometric titration, CD spectroscopy, and molecular docking. Dye **26** was found to exhibit a large bathochromic shift and a significant decrease in intensity in the absorption spectra along with a significant fluorescence enhancement upon binding to a G-quadruplex DNA, while it demonstrated little changes upon interaction with a duplex DNA. CD studies have shown that dye

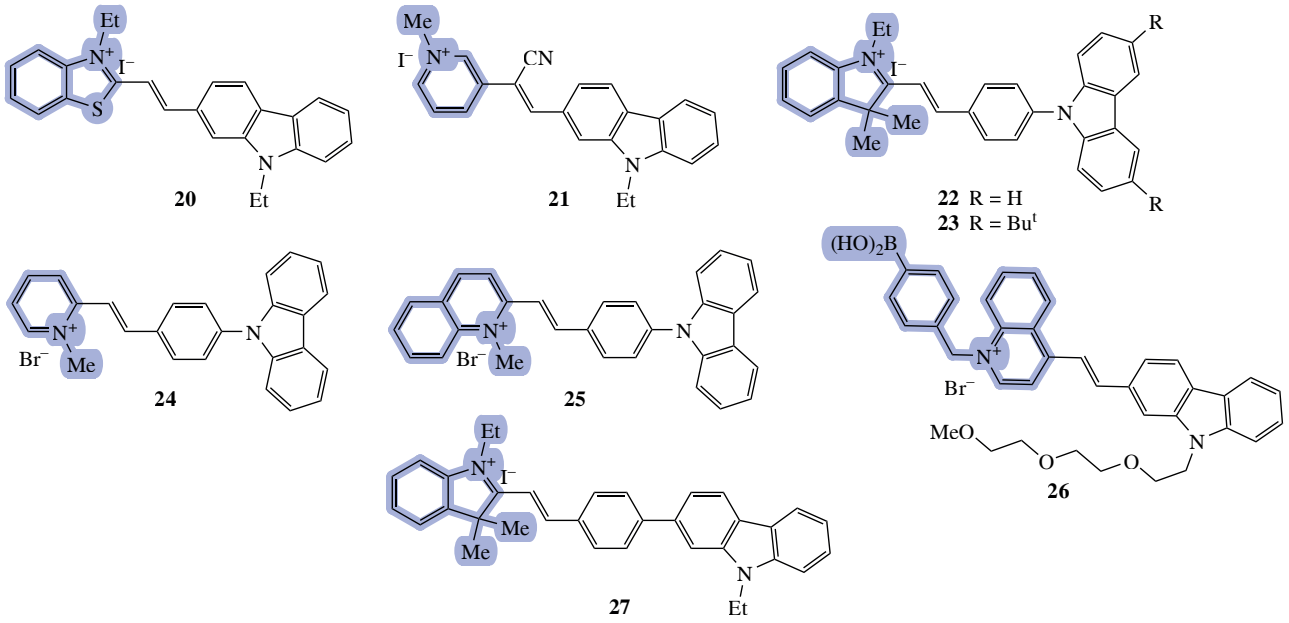

Figure 6 Structures of styryl dyes **20**–**27** containing a carbazole moiety.

26 had the ability to stabilize somewhat the structure of G-quadruplex DNA, mainly by stacking with terminal heterocyclic DNA fragments. Using confocal fluorescence microscopy, localization of the dye in the cytoplasm of living cells was determined.

A two-photon probe **27** (see Figure 6) for the monitoring of mitochondrial viscosity was proposed. The probe demonstrated a significant enhancement of fluorescence intensity as the viscosity of the medium increases.[44] The new probe **27** was used to monitor the changes in mitochondrial viscosity in living systems caused by the presence of mitochondria-damaging monensin or nystatin in real time with high sensitivity. In addition, the probe was capable of visualizing the changes in mitochondrial viscosity during the development of an inflammation process at the cellular and organismal levels in danio fish and mice. It was shown that the changes in mitochondrial viscosity could be observed both in mice with fatty hepatosis and mice with tumors. These studies not only contribute to knowledge about the relationship between the disease and mitochondrial viscosity, but also provide an effective way to diagnose diseases based on changes in mitochondrial viscosity.

The effect of steric factors and electronic properties of heterocycles on the characteristics was estimated using dyes **28**–**36** as examples. The dyes comprise various *N*-quaternary heterocycles based on *o*- and *p*-quinolinium, *o*- and *p*-pyridinium, as well as benzo-annulated five-membered heterocyclic derivatives; all the dyes **28**–**36** feature the same 4-(4-methylpiperazine)phenyl aryl moiety (Figure 7).[45] The results showed that the absorption maximum of the dyes shifts bathochromically in the following series: **36** < **35** < **32** = **30** < **31** < **29** < **28** < **33** < < **34**. It was also found that the Stokes shift (94–203 nm) and fluorescence quantum yield (0.18–2.38 – 10^{-2}) depended on the nature of the *N*-quaternary heterocycle. Dyes **31**–**32**, **35**–**36** containing pyridinium or quinolinium moieties manifest a larger Stokes shift compared to the dyes containing additional heteroatoms, such as oxygen, sulfur, or selenium, within the aza-heterocyclic moiety. Changing the position of substituents at pyridine and quinoline heterocycles from *ortho* to *para* was found to increase significantly the fluorescence quantum yield. The large Stokes shift of the dyes decreases the probability of the self-quenching process, thus increasing the sensitivity of fluorophores as fluorescent probes.

Spectrophotometric studies on the interaction of dyes **28**–**36** with DNA/RNA showed that upon binding to a biomolecule, all the fluorophores exhibited moderate bathochromic and hypochromic shifts in the absorption spectra, a significant increase in fluorescence intensity, small changes in DNA/RNA CD spectra, and minor stabilization of double-stranded polynucleotides in thermal denaturation experiments. Comparison of the binding constants of different dyes with DNA revealed a slightly higher affinity to DNA for dye **34** than for dye **33** and a higher affinity of dyes **28**, **29** and quinolinium dyes **31**, **32** compared to pyridinium dyes **35**, **36**.

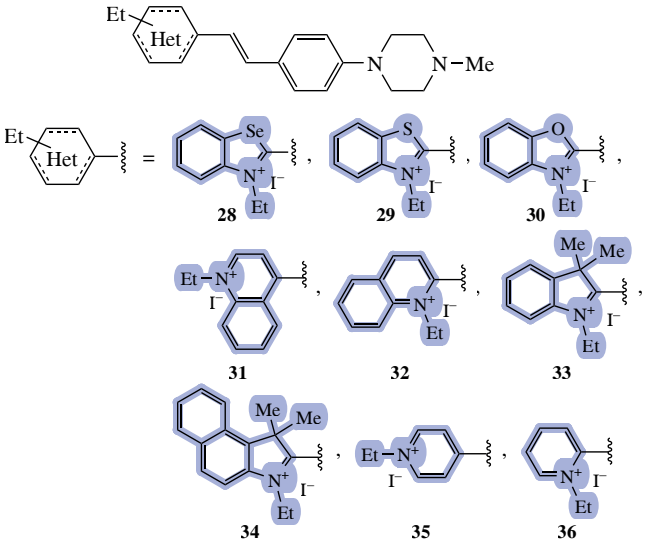

Figure 7 Structures of styryl dyes **28**–**36** based on 4-(4-methylpiperazine)-phenyl.

Most of the dyes in question revealed negligible cytotoxic activity at low concentrations. Only probe **34** had moderate cytotoxicity even at micromolar concentrations, which may be due to the partial intercalation into the DNA/RNA structure. Almost all the dyes showed localization in mitochondria, except for dye **28**, which was localized predominantly in lysosomes, and dye **34**, which showed equal distribution between mitochondria and lysosomes. The observed cytotoxicity of ligand **34**, combined with its easily controlled localization, allowed the authors to propose this dye as a theranostic agent.

A study on phenanthridine dyes **37**–**39** (Figure 8) when the substituents in the donor moiety of the amino group were varied showed that even such small changes in the composition affect the properties exhibited by the compound.[46] The dyes demonstrated broad absorption and emission bands in various solvents with maxima at 411–529 and 623–684 nm and large Stokes shifts of 133–230 nm. They exhibited good stability at physiological pH values (4–9) and were sensitive to the viscosity of the environment. As the viscosity was increased from 0.89 to 856 cP, the fluorescence intensity in glycerol increased 115-fold (dye **37**), 83-fold (dye **38**), or 303-fold (dye **39**) compared to that in the aqueous solutions. The best performance in biological experiments was demonstrated by dye **37**; it showed high photostability, low cytotoxicity, and localization in the mitochondrial region. In experiments with HeLa cells, the authors confirmed that dye **37** could detect changes in mitochondrial viscosity during autophagy induced by rapamycin and nystatin.

By varying the donor amino group at position 4 of the aryl moiety, a large series of hemicyanine dyes based on pyridine **40a**–**46a** and quinoline **40b**–**46b** was synthesized (Figure 9).[47] The dyes manifested broad absorption bands in the region from 400 to 700 nm, with the absorption maxima of quinolinium derivatives **40b**–**46b** shifted by 40–70 nm to the red region relative to the pyridinium analogs **40a**–**46a**. The dyes had very large Stokes shifts (147–242 nm) and rather low fluorescence quantum yields (0.05–1.68%). The fluorescence intensity increased in aprotic and viscous media. Thus, the dyes were medium-sensitive, therefore the authors further studied the interaction of dyes with DNA biomolecules. The interaction of a dye with DNA resulted in a significant increase in fluorescence intensity. The effect of the structure was demonstrated in models of binding to DNA. According to CD spectroscopy data, dyes **41a**–**43a** and **45a**–**46a** of the pyridine series bind to DNA by association with the DNA side surface, along which the phosphate groups are located. Changes typical of intercalation

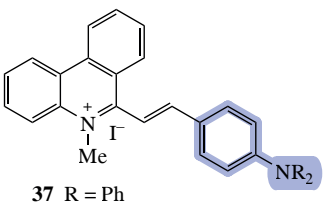

37 R = Ph
38 R = Et
39 R + R = $(CH_2)_2O(CH_2)_2$

Figure 8 Structures of styryl dyes **37**–**39** based on phenanthridine.

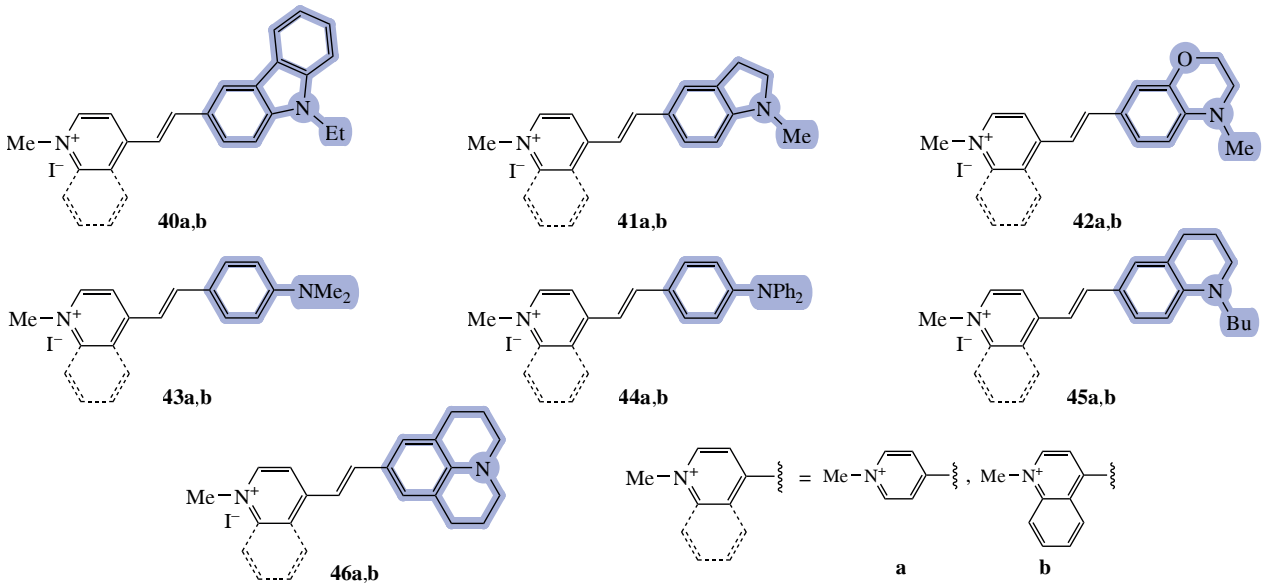

Figure 9 Structures of styryl dyes based on pyridine (**40a**–**46a**) and quinoline (**40b**–**46b**).

binding were observed in the CD spectra of dye **40a**. In the case of dye **44a**, the emergence of exciton bands was observed. This usually correlates with the formation of chiral aggregates on the surface of the DNA chain. For quinolinium derivatives **40b**–**46b**, the formation of aggregates in the DNA body was also observed. In biological experiments, all the dyes showed low cytotoxic activity and localization in cell mitochondria.

Dyes **41a** and **45a** demonstrated the most significant fluorescence enhancement with increasing viscosity. They were further studied in more detail as sensors to visualize viscosity changes in mitochondria using Fluorescence Lifetime Imaging Microscopy (FLIM).[48] The authors stated that dyes **41a** and **45a** could be used to identify pathological cell states by demonstrating fluorescence changes during mitophagy. It was shown, however, that the observed fluorescence response in mitochondria was caused not only by the viscosity of the medium, but also by interactions with cell components, such as proteins and nucleic acids.

Detailed studies on the interaction of *N*-methyl- (**47**) and *N*-[3-(pyridin-1-ium-1-yl)propyl]- (**48**) pyridinium dyes with a DNA biomolecule showed that, despite the structural similarities, the dyes were bound to DNA by different mechanisms (Figure 10).[49] According to CD spectroscopy, compound **47** interacted with DNA by intercalation, whereas compound **48** interacted by embedding into a small groove. Thus, small modifications in one of the substituents in the dye can lead to significant changes in the mechanism of its interaction with the biomolecule.[50]

Bisstyryl dyes are also used as ligands for binding to nucleic acids.[51–53] As a rule, bisstyryl dyes form aggregates in the minor groove of DNA.[52] It has been shown[53] that asymmetric bisstyryl dyes **49** and **50** (Figure 11) form rather strong complexes both with DNA (ct-DNA) (log K_{11} = 5.4 for dye **49** and 5.3 for dye **50**) and RNA (cl-RNA) (log K_{11} = 4.7 for dye **49** and 4.9 for dye **50**). The compounds show a 151-fold (for dye **49**) and 118-fold (for

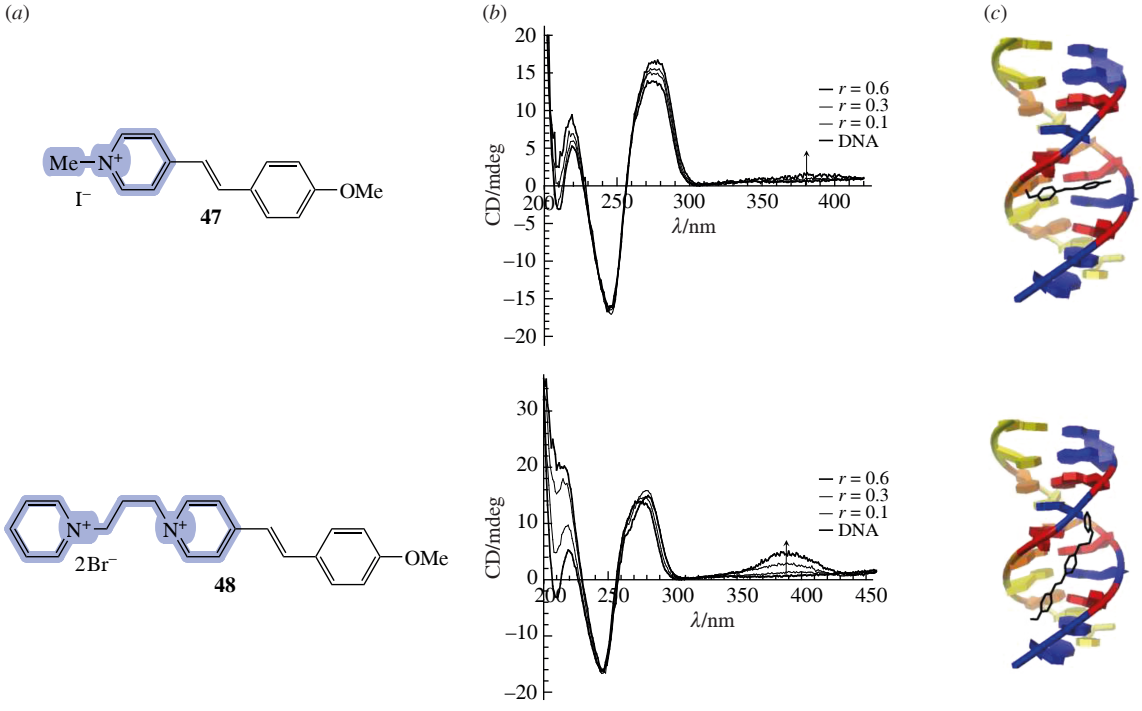

Figure 10 (*a*) Structures of styryl dyes **47** and **48** based on pyridine; (*b*) circular dichroism spectroscopy spectra for dye complexes with DNA; (*c*) models of dye–DNA interaction.

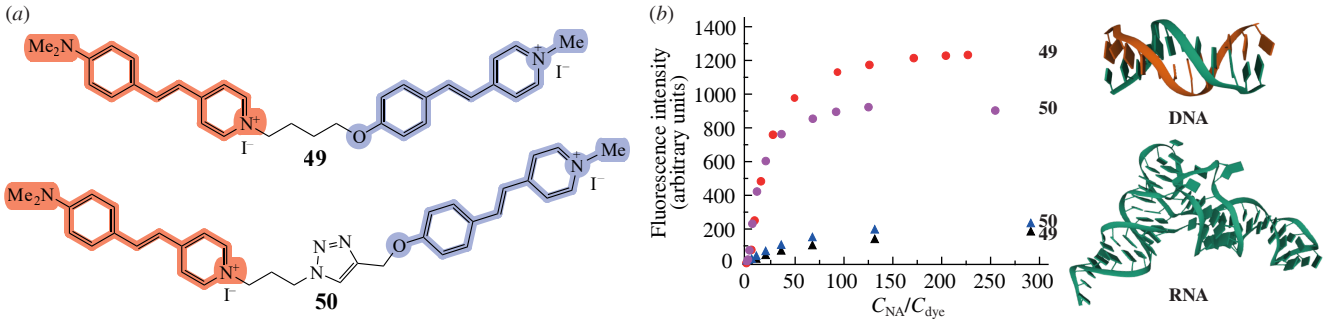

Figure 11 (*a*) Structures of bisstyryl dyes **49** and **50**; (*b*) change in fluorescence intensity of the dye with an increase in DNA/RNA concentration in solution.

dye **50**) fluorescence enhancement in DNA solutions, whereas the enhancement was significantly smaller (23-fold for dye **49** and 36-fold for dye **50**) in the presence of RNA. When fixed A549 cells were stained, both dyes showed localization in the nucleus. Experiments on the cleavage of complexes of fluorophores **49** and **50** with NA by DNase and RNase revealed that dye **49** loses fluorescence upon DNA cleavage, but, in contrast, it retains its fluorescence level upon RNA cleavage, *i.e.*, this dye can be used to determine nuclear DNA in the presence of RNA. The fluorescence response of compound **50** in cells to the presence of DNase and RNase was not as pronounced.

Polymethine dyes

Hemicyanine dyes with two or more multiple bonds in the linker structure belong to the subclass of polymethine dyes. Due to the high conjugation of double bonds is these dyes, they generally have longer-wavelength absorption and fluorescence maxima. Based on the heterocyclic compounds described in the above chapter dealing with the synthesis and study of styryl dyes, a similar series of polymethine dyes have been reported in the literature. Strong electron-donating groups (NEt_2, NMe_2) were incorporated into the structures of benzothiazolium dyes to improve the ICT process.[54] Probes **51**–**56** (Figure 12) demonstrated good photophysical characteristics for practical applications, including emission in the NIR region, large Stokes shifts, absence of molecular aggregation, and solvatochromism. When these probes were used to stain oligodendrocytes (a class of glial cells in the central nervous system), they demonstrated localization in the mitochondria of living cells even at low concentrations (0.2 μM). Of the probes studied, dye **55** ($\lambda_{max}^{abs} \approx 620$ nm, $\lambda_{max}^{fluor} \approx 702$ nm) is of particular interest because of its large Stokes shift, bright fluorescence upon binding to mitochondria, high biocompatibility, and rapid staining.

A relevant problem in bioimaging is the detection of the aggregation of β-amyloid being a causal factor in the development of Alzheimer's disease.[55] During disease progression, β-amyloid is deposited between neurons and exerts a toxic effect on them. Therefore, the use of fluorescent agents to visualize the aggregation processes of β-amyloid would allow disease development at earlier stages. Three hemicyanine dyes **57**–**59** (see Figure 12) were proposed for visualization of β-amyloid.[20] The dyes exhibited emission bands ranging from 593 to 803 nm in phosphate buffer solution and large Stokes shifts (64–285 nm from **57** to **59**). Two hemicyanine dyes, **57** and **58**, showed an increase in fluorescence intensity with increasing solvent viscosity. The fluorescence intensity of dye **59** is quite low, which ruled out the possibility of using this compound for further biological experiments. The authors further investigated the interaction of dyes **57** and **58** with β-amyloid aggregates. The intense fluorescence response of the dyes to β-amyloid aggregates was due to the inhibition of the formation of twisted TICT states. The dissociation constants of dyes with aggregates were 507.6 ± 94.75 nM for dye **57** and 600.6 ± 94.82 nM for dye **58**. According to the calculations by molecular docking, the enhancement of dye fluorescence upon binding to aggregates was attributed to the fact that the molecules were embedded in the hydrophobic cavities of β-amyloid aggregates. This limited the rotational relaxation of the excited state of the irradiated molecule thus enhancing the fluorescence quantum yield. Further, to improve the passage of the dye through the blood–brain barrier (BBB) and penetration into the brain, bioconjugates of the dye with lactoferrin were obtained. Lactoferrin receptors located on the surface of the brain glial cells can specifically bind lactoferrin and transfer it into the brain by the endocytose process.[56] The bioconjugates obtained demonstrated better biocompatibility than the free dyes **57** and **58**. It was shown in *in vivo* experiments that bioconjugates with

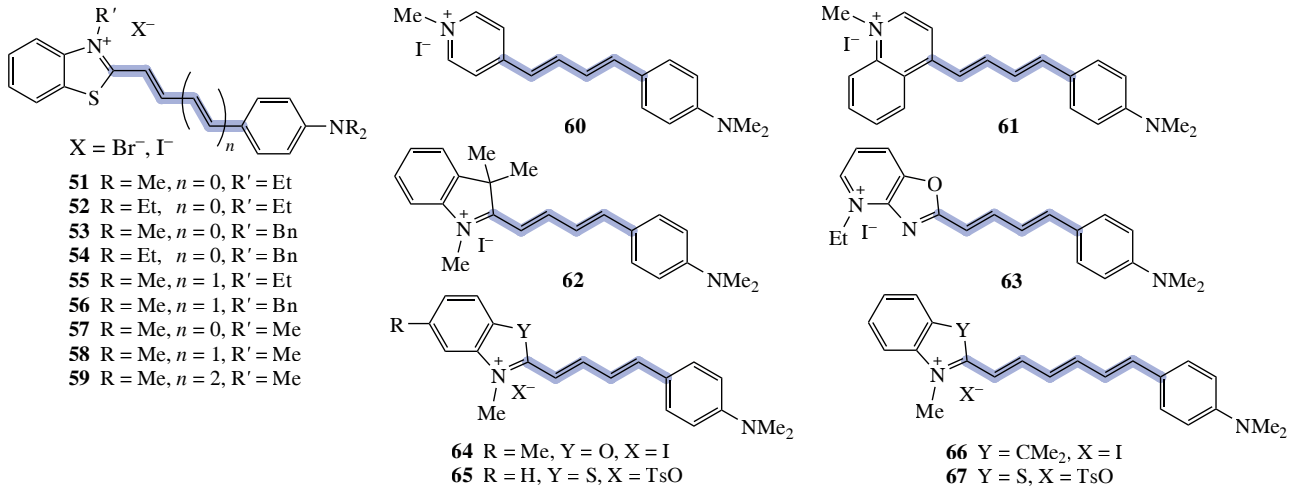

Figure 12 Structures of polymethine dyes **51**–**67**.

dyes **57** and **58** could visualize β-amyloid in the brain of a transgenic mouse with Alzheimer's disease for a longer time (>60 min) than the majority of the known molecular probes.

One more example of polymethine dyes is presented in a work[57] where the optical properties of dyes **60**,**61** (see Figure 12), their affinity to DNA and RNA biomolecules, and their behavior *in vitro* were explored. Upon complexation of the dyes with polynucleotides, a marked fluorescence enhancement was observed (100-fold fluorescence enhancement for dye **61**). In *in vitro* experiments, the dyes demonstrated selective RNA staining, with localization in the cell nucleoli and mitochondria. The *para*-quinolinium derivative **61** showed a moderate antiproliferative effect for two tumor cell lines (A549 and HT-29). Thus, hemicyanine dye **61** of quinoline series is a promising RNA-selective fluorescent probe. It also demonstrates antitumor activity and can therefore be considered as a theranostic agent.

Indolinium polymethine dye **62** (see Figure 12) has been proposed[58] for the selective detection of human serum albumin (HSA). The selectivity of probe **62** was examined in the presence of thiol-containing proteins such as glutathione reductase, hemoglobin, trypsin, DNase, lysozyme, minor thiols such as cysteine, homocysteine, glutathione, dithiothreitol, glucose, and DNA and RNA nucleotides. No significant changes in the dye fluorescence intensity were observed, indicating that probe **62** was selective for HSA among the tested bioanalytes. The selective turn-on fluorescence response of probe **62** in the presence of HSA is due to the restriction of bonds rotation in the dye molecule through hydrophobic interaction with the IIA domain of HSA. The effective interaction between dye **62** and HSA was also confirmed by quantum-chemical calculations. The results suggest that dye **62** is a promising platform for the early diagnosis of HSA-related diseases.

Six polymethine dyes **62**–**67** (see Figure 12) were presented in a work where the heterocyclic moieties in their structures were varied.[19] All the dyes exhibited fluorescence in the range of 600 to 850 nm. Benzothiazolium dye **65** showed better photo- and thermal stability compared to the other dyes in the series. When dye **65** was titrated with DNA and RNA solutions, a strong increase in the emission band from 575 to 850 nm was observed. Biological experiments on living HeLa, KB, and V79 cells showed that dye **65** had greater selectivity for RNA staining and could also be used as a near-infrared fluorescent probe for nuclear imaging of living cells.

Polymethine dyes with rigid moieties in the linker

One of the key issues for hemicyanine dyes with double bonds is their relatively low fluorescence quantum yield due to radiationless relaxation. A common strategy to overcome this limitation is to introduce rigid fragments into the polymethine spacer structure to prevent intramolecular rotation of molecular fragments relative to each other. Thus, the fluorescence quantum yield of such dyes should be higher than that of similar dyes with the same number of double bonds capable of isomerization. Examples of such compounds reported in the literature will be discussed below.

A scientific team from India published an article[59] in which hemicyanine dye **68** (Figure 13) was studied as a fluorescent probe for bioimaging. Studies on the optical properties of the dye in solvents with different polarity and pH showed that the dye was sensitive to local changes in the medium. The dye had an absorption maximum at 590 nm and a fluorescence maximum at 785 nm in aqueous solution, *i.e.* in the NIR range. Upon formation of a complex with a DNA biomolecule, a hypsochromic shift of the fluorescence maximum and a significant increase in the intensity were observed in the emission spectrum, confirming that binding of the dye to the biomolecule occurred. The interaction of the dye with DNA was also accompanied by an increase in the mean fluorescence lifetime.

A series of four indolinine dyes **69**–**72** (see Figure 13) whose polymethine chains included thiophene and pyrrole moieties was developed by researchers from China.[60] They proposed to use these dyes as sensors of β-amyloid aggregation. Due to the long π-conjugated system, the dyes exhibited near-infrared emission ($\lambda_{max}^{fluor} \approx 725$ nm for dyes **69** and **71**; $\lambda_{max}^{fluor} \approx 770$ nm for dyes **70** and **72**). Dye **69** showed the highest increase in fluorescence intensity response to viscosity and to the binding with β-amyloid. The toxicity of dyes **69** and **71** was estimated in biological experiments: the IC_{50} was higher than 20 μM. Co-localization studies revealed that dye **69** was localized in cell mitochondria. *In vitro* experiments in mouse brain slices and brain homogenates demonstrated that dye **69** enabled rapid detection of endogenous β-amyloid aggregates in mice. Hemicyanines **69** and **71** were able to rapidly cross the blood–brain barrier in mice within 10 min. Dye **69** exhibited a 1.56-fold increase in the fluorescence response to β-amyloid plaques in mouse brains, indicating that hemicyanine **69** can distinguish mice with Alzheimer's disease from healthy mice. Therefore, dye **69** is a promising probe for early diagnosis of Alzheimer's disease and for noninvasive evaluation of the efficacy of anti-Alzheimer's drugs *in vivo*.

Hemicyanine dye **73** (see Figure 13) has also been proposed for β-amyloid plaque imaging. The incorporation of a thiophene bridge into the dye structure extended the π-conjugation of the chromophore, which also increased the molecule lipophilicity, thus enhancing its ability to cross the blood–brain barrier. The fluorescence of compound **73** lies in the near-infrared region ($\lambda_{max}^{fluor} \approx 980$ nm in dichloromethane) and is enhanced with an increase in solvent viscosity. Upon binding to β-amyloid fibrils, compound **73** exhibited specific fluorescence enhancement by a factor of 41.8. Moreover, due to its long-wavelength absorption, the compound was capable of penetrating into deeper tissues; the

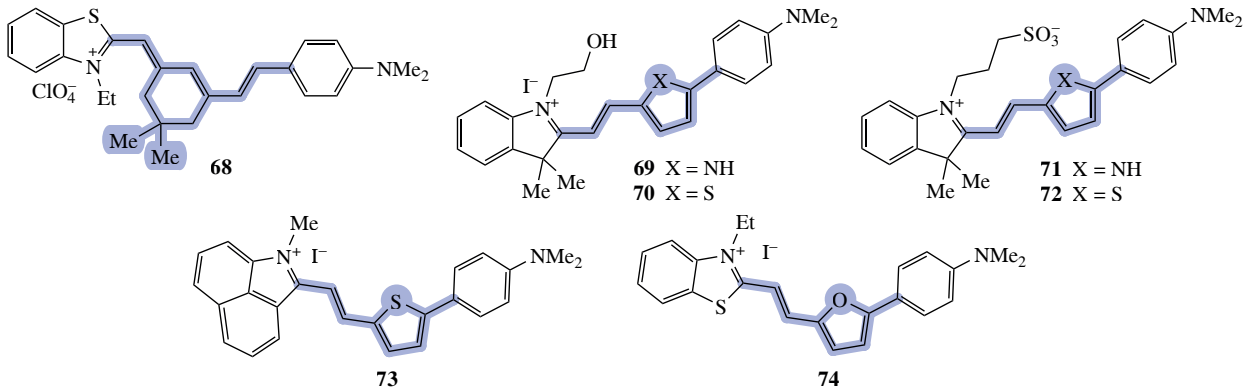

Figure 13 Structures of polymethine dyes **68**–**74** with rigid moieties in the linkers.

dye signal after binding to β-amyloid fibrils was detectable at a tissue depth of 1.5 cm, which is unachievable for dyes absorbing in the visible region. Another advantage of compound **73** is its good blood–brain barrier permeability. Experiments demonstrated the feasibility of *in vivo* fluorescence imaging of β-amyloid plaques using compound **73**.

The furan moiety in compound **74** (see Figure 13) extends the π-conjugation length and provides rigidity to the chromophore.[62] Partial reinforcement of the π-conjugated framework resulted in a significant increase in the fluorescence quantum yield of dye **74** ($\varphi^{fluor} \approx 0.47$ in dichloromethane) along with a large Stokes shift ($\Delta\lambda \approx 109$ nm in dichloromethane). Probe **74** exhibited biocompatibility and capability for long-term imaging, and feasibility of emission excitation by commercially available lasers. Dye **74** was also successfully used for visual identification of mitochondrial dysfunction due to disrupted membrane potential in living cells. Fluorescence confocal microscopy images obtained for NHLF cells stained with probe **74** in the presence of a well-known inhibitor affecting the mitochondrial membrane potential (*e.g.*, carbonyl cyanide 4-(trifluoromethoxy)phenylhydrazone) demonstrated the ability of dye **74** to visually identify cells with mitochondrial membrane potential dysfunction.

Conclusion

There is a growing demand for advanced multicolor fluorescence analysis used not only in various biological studies, but also in medical diagnostic tests for identification of diseases. All these methods require fluorescent markers and probes with diverse characteristics. Although a number of commercial suppliers offer fluorophores and trackers for fluorescence-based assays, the data presented in this review indicate that the range of cellular components, tissues, and organs that can be monitored using fluorescent reagents is constantly expanding. This explains the high research activity in the field of fluorescent dyes which have affinity to biomolecules. The review presents examples of studies on hemicyanine dyes as bioimaging agents. The optical characteristics of this class of dyes cover a broad spectral range (from UV to near-infrared), depending on their structure. Hemicyanine dyes can be used for the detection of biomolecules (DNA, RNA, HSA, *etc.*), for selective staining of cellular organelles (lysosomes, mitochondria, endoplasmic reticulum, *etc.*), and for the recognition of pathological states of cells (mitophagy, β-amyloid aggregation). To simplify interpretation of the large volume of data presented in this review, a summary table has been included to briefly summarize the discussed data (see Online Supplementary Materials). The examples of fluorophores reported in the literature also describe the main structural approaches to their synthesis. Many of these compounds require further optimization to meet the criteria of brightness, absence of photoinduced side processes, high stability under assay conditions, compatibility with lasers and optical filters of research equipment, and photostability.

The work was supported by The Russian Science Foundation (grant no. 21-73-20158-P).

Online Supplementary Materials

Supplementary data associated with this article can be found in the online version at doi: 10.71267/mencom.7826.

References

1 W. E. Moerner and D. P. Fromm, *Rev. Sci. Instrum.*, 2003, **74**, 3597; https://doi.org/10.1063/1.1589587.
2 D. P. Millar, *Curr. Opin. Struct. Biol.*, 1996, **6**, 322; https://doi.org/10.1016/S0959-440X(96)80050-9.
3 C. A. Royer, *Chem. Rev.*, 2006, **106**, 1769; https://doi.org/10.1021/cr0404390.
4 A. Schepartz and R. L. Gonzalez, Jr., *Curr. Opin. Chem. Biol.*, 2011, **15**, 749; https://doi.org/10.1016/j.cbpa.2011.11.001.
5 G. P. C. Drummen, *Molecules*, 2012, **17**, 14067; https://doi.org/10.3390/molecules171214067.
6 S. Munan, Y. T. Chang and A. Samanta, *Chem. Commun.*, 2024, **60**, 501; https://doi.org/10.1039/D3CC04895K.
7 X. Sun, Q. Jiang, Y. Zhang, J. Su, W. Liu, J. Lv, F. Yang and W. Shu, *Eur. J. Med. Chem.*, 2024, **267**, 116195; https://doi.org/10.1016/j.ejmech.2024.116195.
8 P. Luo, M. Wang, W. Liu, L. Liu and P. Xu, *Molecules*, 2022, **27**, 7750; https://doi.org/10.3390/molecules27227750.
9 H. Mustroph, *Dyes Pigm.*, 2023, **208**, 110783; https://doi.org/10.1016/j.dyepig.2022.110783.
10 T. Deligeorgiev, A. Vasilev, S. Kaloyanova and J. J. Vaquero, *Color. Technol.*, 2010, **126**, 55; https://doi.org/10.1111/j.1478-4408.2010.00235.x.
11 R. Putralis, A. Plotniece and K. Pajuste, *Chem. Heterocycl. Compd.*, 2025, **60**, 439; https://doi.org/10.1007/s10593-024-03360-w.
12 Y. Zhang, F. Bu, Y. Zhao, B. Zhao, L. Wang and B. Song, *Anal. Chim. Acta*, 2020, **1098**, 155; https://doi.org/10.1016/j.aca.2019.11.040.
13 H. Li, H. Kim, F. Xu, J. Han, Q. Yao, J. Wang, K. Pu, X. Peng and J. Yoon, *Chem. Soc. Rev.*, 2022, **51**, 1795; https://doi.org/10.1039/D1CS00307K.
14 M. J. Patrick, L. A. Ernst, A. S. Waggoner, D. Thai, D. Tai and G. Salama, *Org. Biomol. Chem.*, 2007, **5**, 3347; https://doi.org/10.1039/B711438A.
15 D. K. Palit, A. K. Singh, A. C. Bhasikuttan and J. P. Mittal, *J. Phys. Chem. A*, 2001, **105**, 6294; https://doi.org/10.1021/jp004142r.
16 I. López-Duarte, P. Chairatana, Y. Wu, J. Pérez-Moreno, P. M. Bennett, J. E. Reeve, I. Boczarow, W. Kaluza, N. A. Hosny, S. D. Stranks, R. J. Nicholas, K. Clays, M. K. Kuimova and H. L. Anderson, *Org. Biomol. Chem.*, 2015, **13**, 3792; https://doi.org/10.1039/C4OB02507E.
17 H. J. Park, C. W. Song, S. Sarkar, Y. W. Jun, Y. J. Reo, M. Dai and K. H. Ahn, *Chem. Commun.*, 2020, **56**, 7025; https://doi.org/10.1039/D0CC01833C.
18 W. Cao, Y. Zhu, F. Wu, Y. Tian, Z. Chen, W. Xu, S. Liu, T. Liu and H. Xiong, *Small*, 2022, **18**, 2204851; https://doi.org/10.1002/smll.202204851.
19 J. T. Miao, C. Fan, R. Sun, Y. J. Xu and J. F. Ge, *J. Mater. Chem. B*, 2014, **2**, 7065; https://doi.org/10.1039/C4TB01218F.
20 L. Ma, S. Yang, Y. Ma, Y. Chen, Z. Wang, T. D. James, X. Wang and Z. Wang, *Anal. Chem.*, 2021, **93**, 12617; https://doi.org/10.1021/acs.analchem.1c02289.
21 H. Wang, J. Y. Zhao, R. Sun and J. F. Ge, *Microchem. J.*, 2025, **212**, 113344; https://doi.org/10.1016/j.microc.2025.113344.
22 *Fluorescent Analogs of Biomolecular Building Blocks: Design and Applications*, eds. M. Wilhelmsson and Y. Tor, Wiley, 2016; https://onlinelibrary.wiley.com/doi/book/10.1002/9781119179320.
23 D. L. Wilson, A. A. Beharry, A. Srivastava, T. R. O'Connor and E. T. Kool, *Angew. Chem., Int. Ed.*, 2018, **57**, 12896; https://doi.org/10.1002/anie.201807593.
24 J. N. Wilson and E. T. Kool, *Org. Biomol. Chem.*, 2006, **4**, 4265; https://doi.org/10.1039/B612284C.
25 C. S. Abeywickrama, K. A. Bertman, L. J. Mcdonald, N. Alexander, D. Dahal, H. J. Baumann, C. R. Salmon, C. Wesdemiotis, M. Konopka, C. A. Tessier and Y. Pang, *J. Mater. Chem. B*, 2019, **7**, 7502; https://doi.org/10.1039/C9TB01672D.
26 C. S. Abeywickrama, H. J. Baumann and Y. Pang, *J. Fluoresc.*, 2021, **31**, 1227; https://doi.org/10.1007/s10895-021-02786-1.
27 J. Zhou, W. Shi, L.-H. Li, Q.-Y. Gong, X.-F. Wu, X.-H. Li and H.-M. Ma, *Chem. – Asian J.*, 2016, **11**, 2719; https://doi.org/10.1002/asia.201600012.
28 C. S. Abeywickrama, *Chem. Commun.*, 2022, **58**, 9855; https://doi.org/10.1039/D2CC03880C.
29 C. S. Abeywickrama, H. J. Baumann, K. A. Bertman, B. Corbin and Y. Pang, *Biosensors*, 2022, **12**, 504; https://doi.org/10.3390/bios12070504.
30 C. S. Abeywickrama, Y. Li, A. Ramanah, D. N. Owitipana, K. J. Wijesinghe and Y. Pang, *Sens. Actuators, B*, 2022, **368**, 132199; https://doi.org/10.1016/j.snb.2022.132199.
31 A. A. Vasilev, M. Miteva, N. Ishkitiev, M. Dragneva, L. Topalova and M. I. Kandinska, *Molbank*, 2022, M1392; https://doi.org/10.3390/M1392.
32 H. Huang, W. Liu, X.-J. Liu, Y.-Q. Kuang and J.-H. Jiang, *Talanta*, 2017, **168**, 203; https://doi.org/10.1016/j.talanta.2017.03.043.

33 B.-Y. Zhang, X.-F. Zhang, X.-Y. Ma, D.-W. Yang, H.-X. Sun, Y.-L. Tang and L. Shi, *J. Org. Chem.*, 2023, **88**, 9959; https://doi.org/10.1021/acs.joc.3c00715.

34 B.-Y. Zhang, P. Wang, L. Shi, X.-Y. Ma, J.-K. Xi and X.-F. Zhang, *Microchem. J.*, 2023, **193**, 109085; https://doi.org/10.1016/j.microc.2023.109085.

35 J.-Y. Zhao, G. Zhang, H.-C. Hao, R. Sun, Y.-J. Xu and J.-F. Ge, *Sens. Actuators, B*, 2024, **401**, 135010; https://doi.org/10.1016/j.snb.2023.135010.

36 H. Ma, W.-P. Ni, Q. Lin, R. Sun and J.-F. Ge, *Analyst*, 2025, **150**, 642; https://doi.org/10.1039/d4an01450b.

37 G. Hao, J. Sun and C. Wei, *Bioorg. Med. Chem.*, 2018, **26**, 285; https://doi.org/10.1016/j.bmc.2017.11.044.

38 X.-F. Zhang, H.-J. Zhang, J.-F. Xiang, Q. Li, Q.-F. Yang, Q. Shang, Y.-X. Zhang and Y.-L. Tang, *J. Mol. Struct.*, 2010, **982**, 133; https://doi.org/10.1016/j.molstruc.2010.08.018.

39 C.-C. Chang, J.-Y. Wu and T.-C. Chang, *J. Chin. Chem. Soc.*, 2003, **50**, 185; https://doi.org/10.1002/jccs.200300026.

40 L.-N. Zhu, S.-J. Zhao, B. Wu, X.-Z. Li and D.-M. Kong, *PLoS One*, 2012, **7**, e35586; https://doi.org/10.1371/journal.pone.0035586.

41 K. Zhou, M. Ren, B. Deng and W. Lin, *New J. Chem.*, 2017, **41**, 11507; https://doi.org/10.1039/C7NJ02270K.

42 M.-Q. Wang, G.-Y. Ren, S. Zhao, G.-C. Lian, T.-T. Chen, Y. Ci and H.-Y. Li, *Spectrochim. Acta, Part A*, 2018, **199**, 441; https://doi.org/10.1016/j.saa.2018.03.083.

43 J. Li, Q. Yang, L. Zhao, M. Xu and H. Zhang, *Tetrahedron Lett.*, 2021, **70**, 153004; https://doi.org/10.1016/j.tetlet.2021.153004.

44 J. Yin, M. Peng and W. Lin, *Anal. Chem.*, 2019, **91**, 8415; https://doi.org/10.1021/acs.analchem.9b01293.

45 I. Čipor, A. Kurutos, G. M. Dobrikov, F. S. Kamounah, D. Majhen, D. Nestić and I. Piantanida, *Dyes Pigm.*, 2022, **206**, 110626; https://doi.org/10.1016/j.dyepig.2022.110626.

46 H.-X. Wang, J.-Y. Zhao, H. Wang, H. Ma, J. F. Ge and R. Sun, *Dyes Pigm.*, 2025, **232**, 112479; https://doi.org/10.1016/j.dyepig.2024.112479.

47 A. S. Efimova, M. A. Ustimova, N. S. Chmelyuk, M. A. Abakumov, Y. V. Fedorov and O. A. Fedorova, *Biosensors*, 2023, **13**, 734; https://doi.org/10.3390/bios13070734.

48 A. S. Efimova, M. A. Ustimova, A. Y. Frolova, V. I. Martynov, S. M. Deyev, Y. V. Fedorov, O. A. Fedorova and A. A. Pakhomov, *Opt. Mater. (Amsterdam, Neth.)*, 2025, **159**, 116517; https://doi.org/10.1016/j.optmat.2024.116517.

49 M. A. Ustimova, P. A. Chernikova, N. E. Shepel, Yu. V. Fedorov and O. A. Fedorova, *Mendeleev Commun.*, 2020, **30**, 217; https://doi.org/10.1016/j.mencom.2020.03.029.

50 D. V. Berdnikova, N. I. Sosnin, O. A. Fedorova and H. Ihmels, *Org. Biomol. Chem.*, 2018, **16**, 545; https://doi.org/10.1039/C7OB02736B.

51 A. Y. Lebedeva, O. A. Fedorova, V. B. Tsvetkov, V. Y. Grinberg, N. V. Grinberg, T. V. Burova, A. S. Dubovik, K. K. Babievsky and Y. V. Fedorov, *Dyes Pigm.*, 2018, **157**, 80; https://doi.org/10.1016/j.dyepig.2018.04.038.

52 M. A. Ustimova, Y. V. Fedorov, V. B. Tsvetkov, S. D. Tokarev, N. A. Shepel and O. A. Fedorova, *J. Photochem. Photobiol., A*, 2021, **418**, 113378; https://doi.org/10.1016/j.jphotochem.2021.113378.

53 M. A. Ustimova, Y. V. Fedorov, N. S. Chmelyuk, M. A. Abakumov and O. A. Fedorova, *Spectrochim. Acta, Part A*, 2022, **279**, 121446; https://doi.org/10.1016/j.saa.2022.121446.

54 C. S. Abeywickrama, H. J. Baumann, N. Alexander, L. P. Shriver, M. Konopka and Y. Pang, *Org. Biomol. Chem.*, 2018, **16**, 3382; https://doi.org/10.1039/C8OB00327K.

55 C. A. Lane, J. Hardy and J. M. Schott, *Eur. J. Neurol.*, 2018, **25**, 59; https://doi.org/10.1111/ene.13439.

56 J. Nicolas, S. Mura, D. Brambilla, N. Mackiewicz and P. Couvreur, *Chem. Soc. Rev.*, 2013, **42**, 1147; https://doi.org/10.1039/C2CS35265F.

57 A. Cesaretti, E. Calzoni, N. Montegiove, T. Bianconi, M. Alebardi, M. A. La Serra, G. Consiglio, C. G. Fortuna, F. Elisei and A. Spalletti, *Int. J. Mol. Sci.*, 2023, **24**, 4812; https://doi.org/10.3390/ijms24054812.

58 S. I. Reja, I. A. Khan, V. Bhalla and M. Kumar, *Chem. Commun.*, 2016, **52**, 1182; https://doi.org/10.1039/C5CC08217J.

59 S. Udayan, V. K. Ramachandran, M. Sebastian, P. Chandran, V. P. N. Nampoori and S. Thomas, *Opt. Mater. (Amsterdam, Neth.)*, 2017, **69**, 49; https://doi.org/10.1016/j.optmat.2017.04.016.

60 W. Wang, Z. Mo, L. Han, H. Zuo, Y. Chen, Y. Fang, X. Li, K. Wang and J. Pan, *Eur. J. Med. Chem.*, 2025, **281**, 11700; https://doi.org/10.1016/j.ejmech.2024.117001.

61 J. Miao, M. Miao, Y. Jiang, M. Zhao, Q. Li, Y. Zhang, Y. An, K. Pu and Q. Miao, *Angew. Chem., Int. Ed.*, 2023, **62**, e202216351; https://doi.org/10.1002/anie.202216351.

62 K. A. Bertman, C. S. Abeywickrama and Y. Pang, *ChemBioChem*, 2022, **23**, e202100516; https://doi.org/10.1002/cbic.202100516.

Received: 15th May 2025; Com. 25/7826